To be submitted to *Atmospheric Chemistry and Physics*

Supplementary material to: In situ observations of gravity waves over tropical cyclone Hinnamnor (2022) suggest that TC gravity wave amplitudes are underestimated in ERA5 reanalysis

Carly KleinStern[1], Benjamin Clouser[2], Thaopaul Bui[3, 4], Jonathan Dean-Day[3, 4], Adrien Desmoulin[2], James Franke[2], Hisashi Nakamura[5], Rei Ueyama[3], Shingo Watanabe[6,7], and Elisabeth Moyer[2]

[1]University of Chicago, Dept. of Physics, Chicago, IL, USA 60637
[2]University of Chicago, Dept. of the Geophysical Sciences, Chicago, IL, USA 60637
[3]NASA Ames Research Center, Moffett Field, CA, USA 94035
[4]Bay Area Environmental Research Institute, Moffett Field, CA, USA 94035
[5]Research Center for Advanced Science and Technology, The University of Tokyo, Tokyo, Japan
[6]Japan Agency for Marine-Earth Science and Technology (JAMSTEC), Yokohama, Kanagawa, Japan
[7]Advanced Institute for Marine Ecosystem Change (WPI-AIMEC), Tohoku University, Sendai, Miyagi, Japan

Correspondence: C. KleinStern, cckleinstern@uchicago.edu; E. Moyer, moyer@uchicago.edu

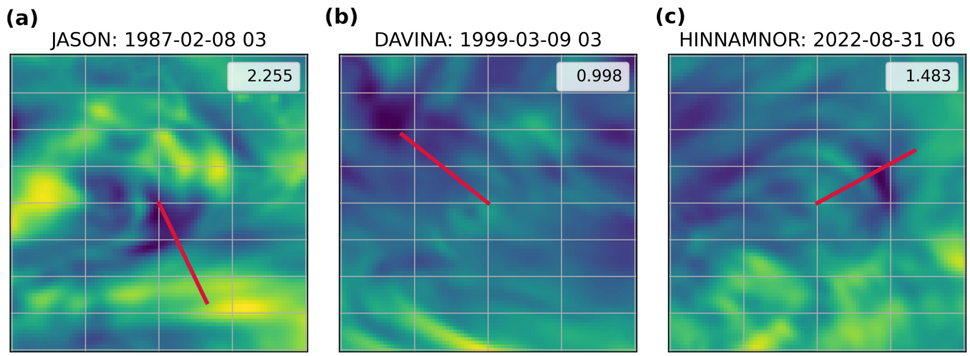

Figure S1. Gravity waves in ERA5 temperature fields at 70 hPa above 3 cyclones overflown by research aircraft: **a)** TC Jason (Eastern Australia) on 8 Feb. 1987, **b)** TC Davina (South Indian ocean basin) on 9 Mar. 1999, and **c)** TC Hinnamnor (Western Pacific basin) on 31 Aug. 2022. Each field is 20 deg $\times$ 20 deg, and wihtout background subtraction. Red line shows the transect used to calculating GW amplitudes and inset text is that amplitude in Kelvin, as our trimmed metric (roughly one-third of the peak-to-peak value). Jason and Davina show anisotropic or muted patterns in ERA5 at the time of overflight but exhibit clearer spiral gravity wave activity at other times.

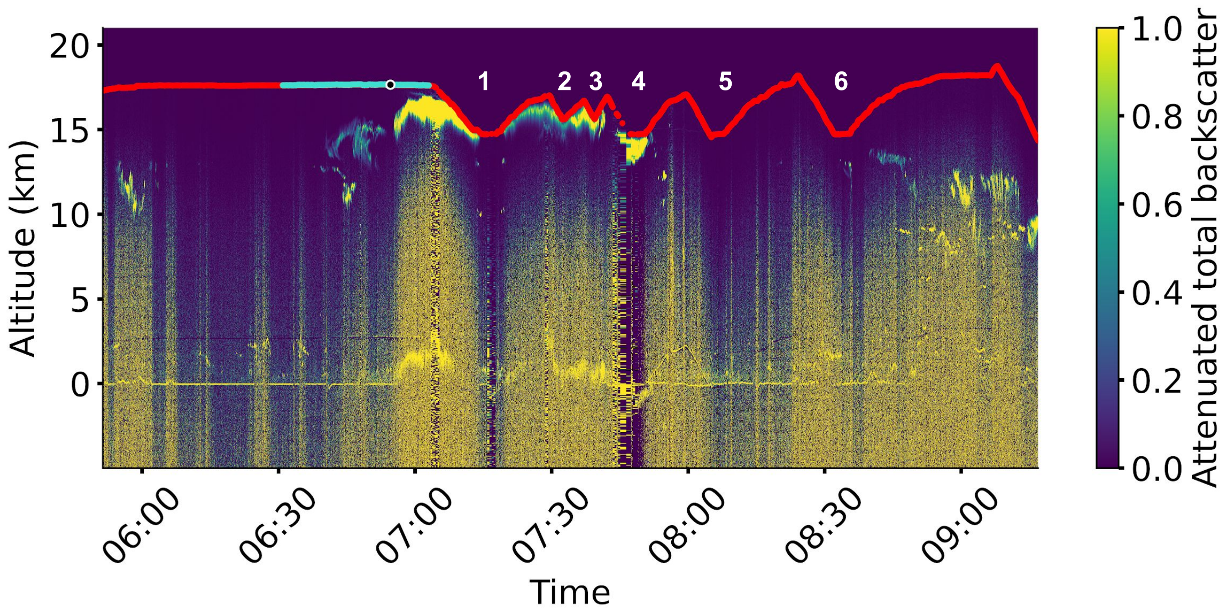

Figure S2. Aircraft altitude on the 31 Aug. 2022 flight overlaid on downwards-looking cloud lidar data taken from the aircraft by the Roscoe instrument. Dives are numbered in white to give flight context, but this work focuses on the level flight leg between 06:00 UTC and 07:00 UTC, in particular the turquoise portion of that leg. The black dot shows the coldest temperature seen during that period. This section of the flight occurred in clear air. Below the flight altitude there is a convective arm of the TC (clouds near 15 km altitude) and TC shield (thick cloud near 16 km). There is no evidence of in situ cirrus cloud decks formed in the cold phase of the gravity wave. As the plane dives into the TC on Dives 1–4, attenuated total backscatter greatly increases, consistent with Himawari cloud top measurements (Fig. 1)

.

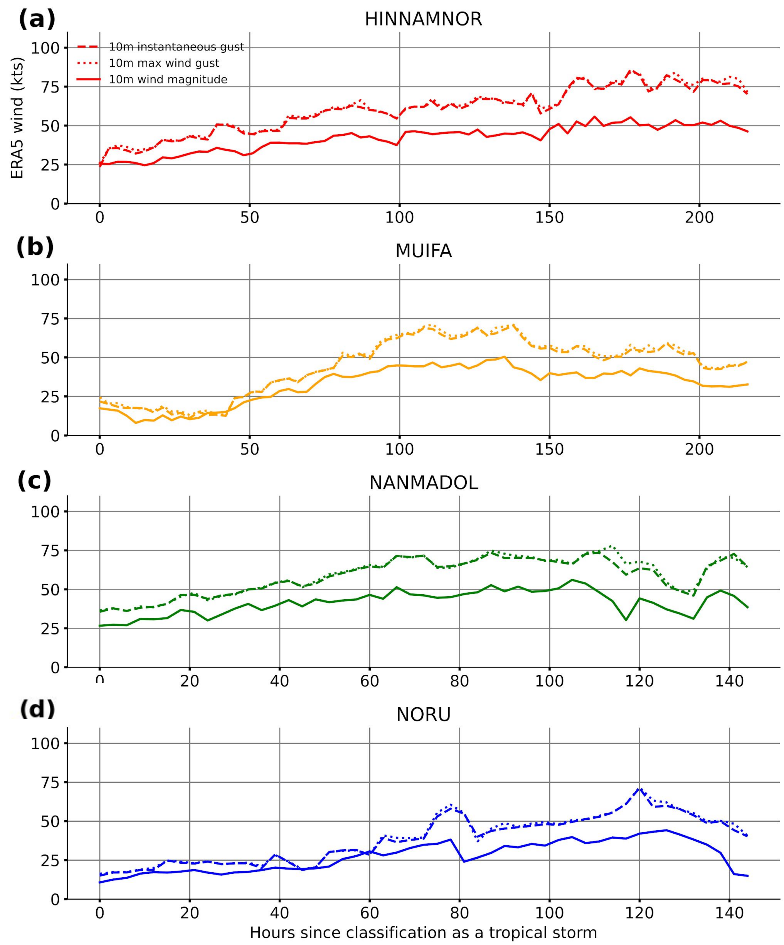

Figure S3. Instantaneous 10 meter wind gust, max 10 meter wind gust, and 10 meter averaged wind magnitude for the four storms in 2022 from our sample: **a)** Hinnamnor; **b)** Muifa; **c)** Nanmadol; and **d)** Noru. The wind gusts are reported over 3 second intervals. As expected, the max 10 meter wind gust is greater than or equal to the instantaneous 10 meter wind gust. For the subsequent figures in this paper, we show 10 meter max wind gusts.

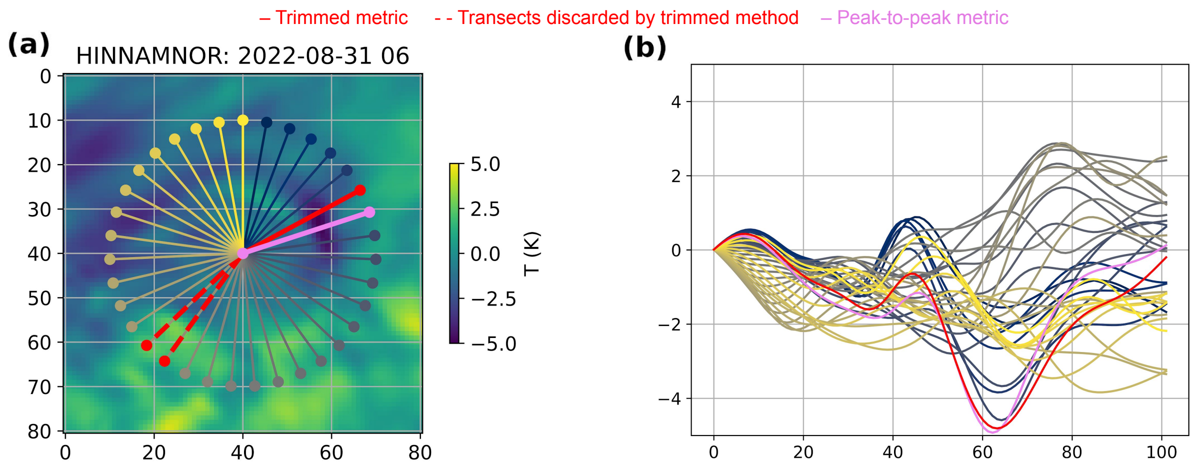

Figure S4. The “transect method" for determining the trimmed and peak-to-peak metric values of ERA5 temperature for each time step of each storm, using Hinnamnor on 31 Aug. 2022 at 06:00 as an example. **a)** we take transects at 10 deg intervals. The solid red line plots the chosen trimmed transect larger than approximately 95 % of all transects (the dashed red lines show the two transects discarded), and the solid pink line shows the chosen peak-to-peak transect. The x and y axes are in pixels. **b)** using bilinear interpolation, we create a line plot of the temperature along each transect.

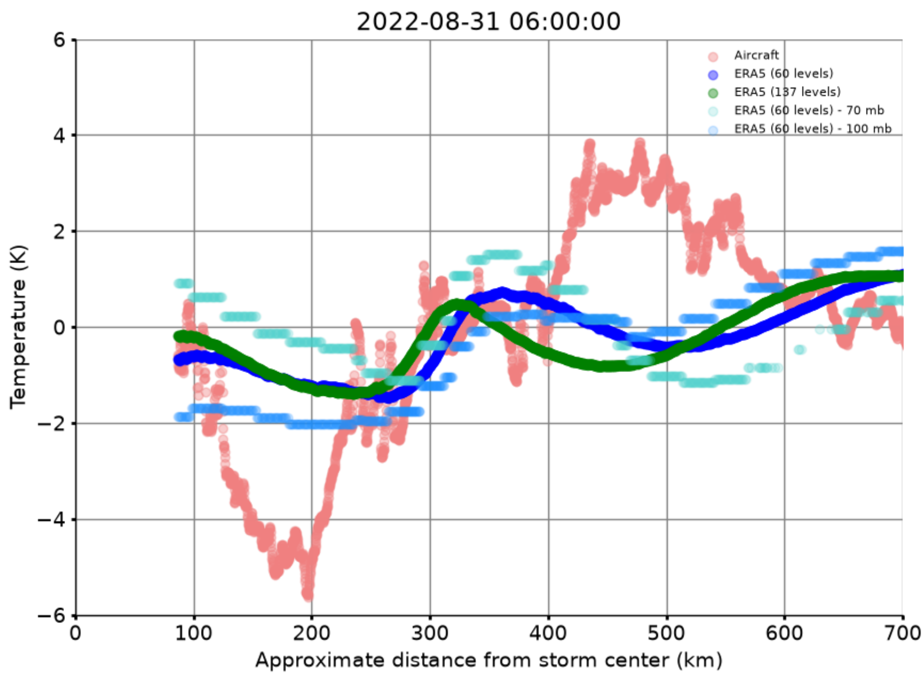

Figure S5. Temperature perturbations along the flight track near TC Hinnamnor on 31 Aug. 2022 in in situ measurements (red, 87 hPa) and in reanalysis interpolated to the flight track: ERA5 60-level (blue) and 137-level (green). In turquoise and light blue is 60-level ERA5 data at 70 hPa and 100 hPa, respectively (bracketing the flight level), in order to show that the interpolated ERA5 data is not egregiously smearing the gravity wave being studied. Perturbations are computed as the difference from the mean temperature over this portion of the level flight leg.

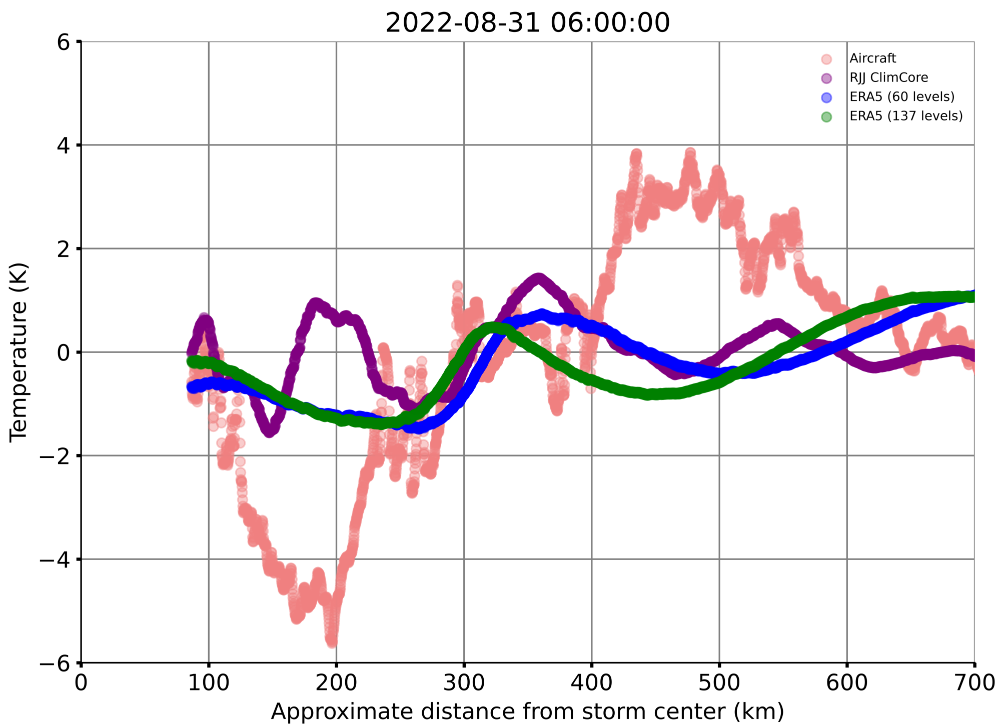

Figure S6. Temperature perturbations along the flight track near TC Hinnamnor on 31 Aug. 2022 in in situ measurements (red, 87 hPa) and 60-level ERA5 reanalysis interpolated to the flight track (blue), 137-level ERA5 reanalysis interpolated to flight track (green), and RRJ-ClimCORE 5-km reanalysis interpolated to the flight track (purple). Perturbations are computed as the difference from the mean temperature over this portion of the level flight leg. Gravity waves in ERA5 reanalysis shows smaller amplitudes and shorter wavelengths than in situ data, with RRJ-ClimCORE reanalysis showing max perturbations of ∼3 K and shorter wavelengths than ERA5 in this specific case.

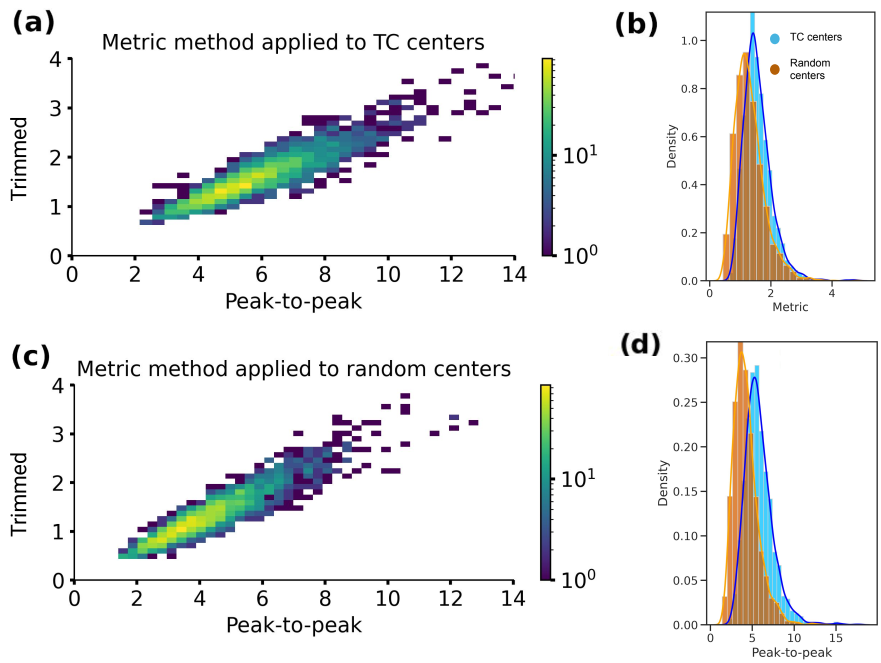

Figure S7. Using the method described in Sect. 2.4, but applied to random latitude/longitude pairs chosen within the confines of the WP basin, which we use as our “storm centers" in ERA5. Does our method produce a unique distribution of peak-to-peak vs trimmed metric values when applied to storms vs random centers in ERA5 reanalysis? From visual inspection of these random snapshots, we identify spiral/concentric structures nearby to the chosen random center point in 30 % of the sample, much lower than the 94 % identified around known TCs. **a), c)** density map of trimmed metric vs peak-to-peak metric for TC centers and random centers, respectively. **b), d)** 1D histograms and probability density function for TC centers (blue) vs random centers (pink), for both trimmed and peak-to-peak methods, respectively. When applied to snapshots containing actual storms, we see an overlap in distributions but overall larger median values for both trimmed and peak-to-peak metric values: 1.49 K vs 1.23 K and 5.53 K vs 4.01 K, respectively. The slopes of the plots are $m = 0.25, 0.3$ for TC vs random centers, respectively. For TC centers, the means of the distributions are higher for both methods.

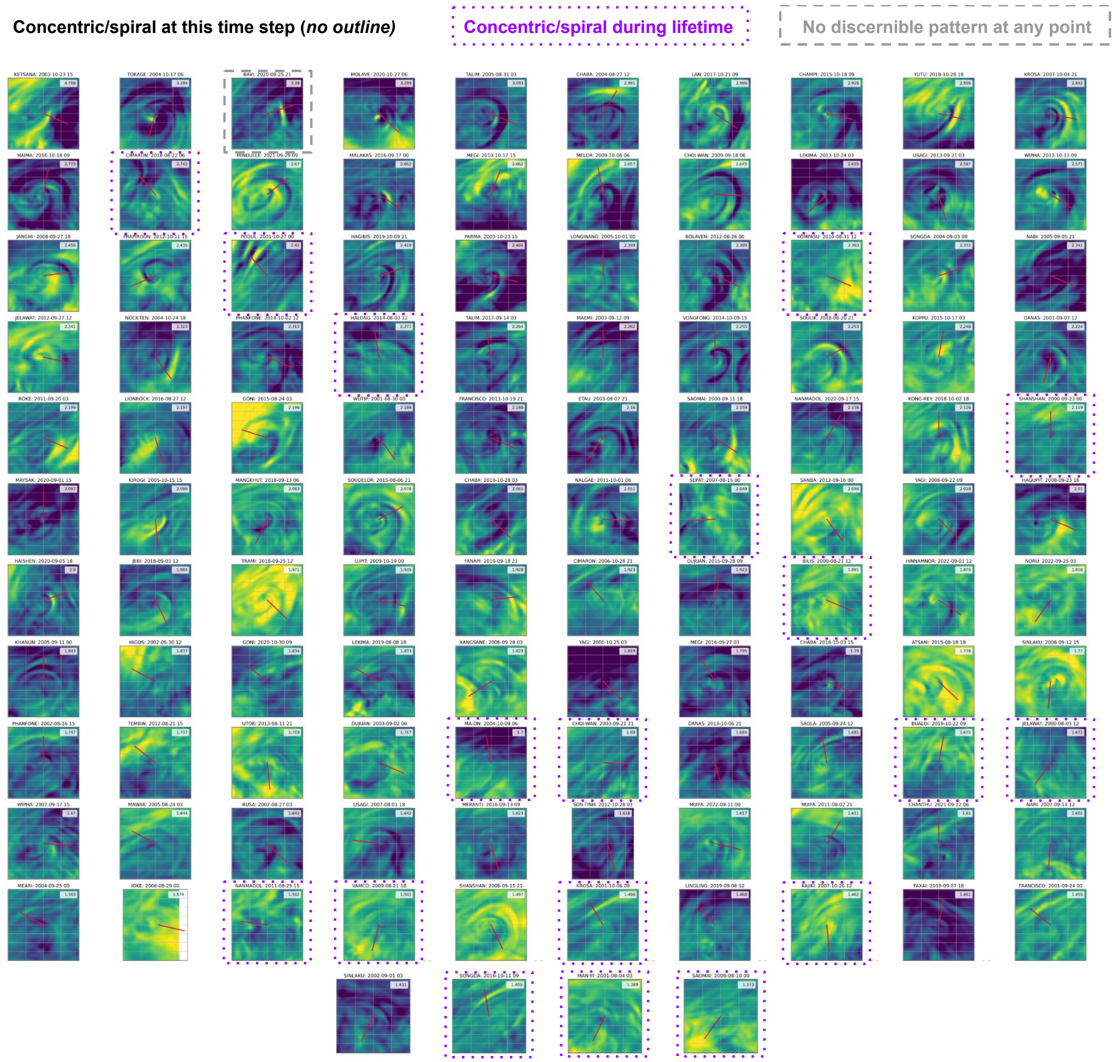

Figure S8. Lifetime strongest GW activity trimmed metric snapshot for each storm in our subset (ERA5, 70 hPa), as chosen by our the trimmed metric. No outline denotes near-concentric/ spiral structure, purple (dotted) shows storms with near-concentric/ spiral structure at some point in their lifetimes, grey (dashed) shows storms with no visibly discernible pattern at any point in their lifetime.

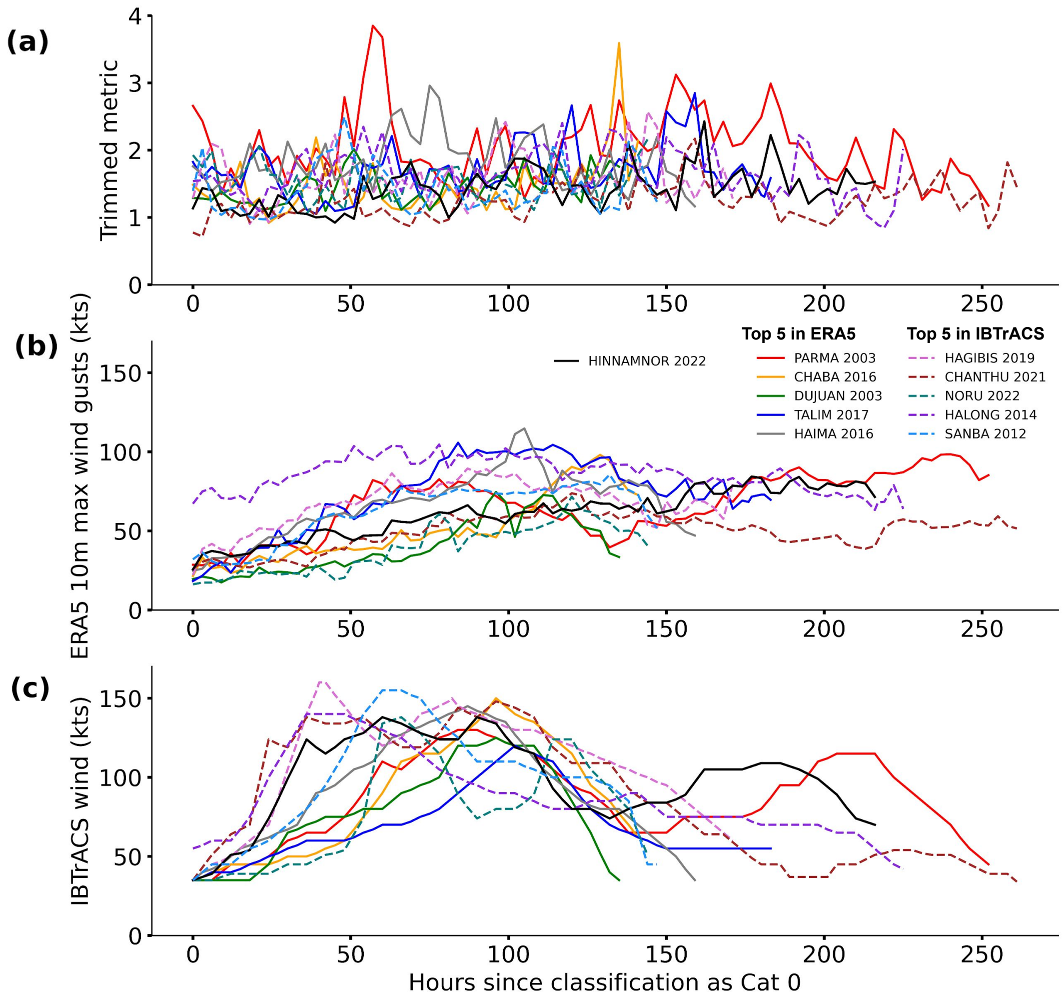

Figure S9. a) Trimmed metric (computed from ERA5 reanalysis), **b)** ERA5 10 meter max wind gusts, and **c)** IBTrACS winds for the 5 storms which show the largest wind change in 24 h, and Hinnamnor. Solid lines represent storms with the largest wind change (intensifying) in ERA5, dashed lines are for storms with tfhe largest wind change in IBTrACS. Hinnamnor shows strong intensification but is not an outlier.

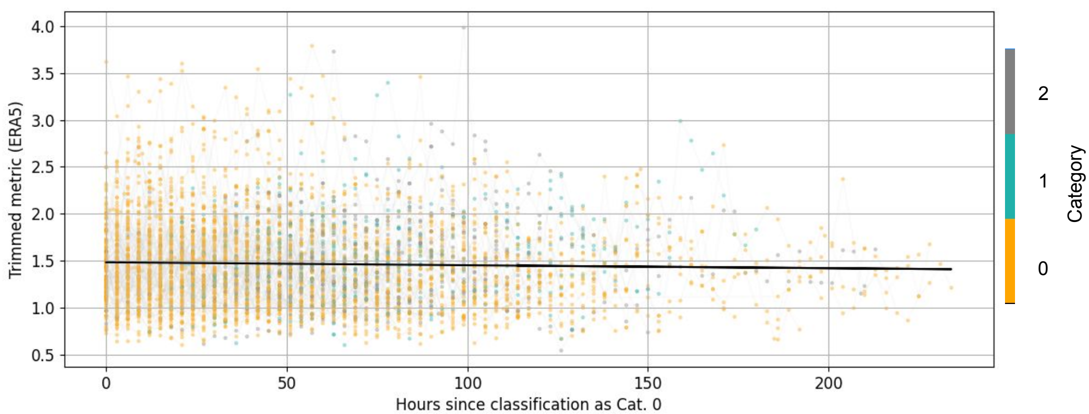

Figure S10. Comparison of the temporal evolution of gravity wave activity derived from ERA5 for storms that never reach Category 3 during their lifetime (n=181). There is a slight downwards trend in storm GW activity during lifetime for overall weaker storms. The black line shows the line of best fit through all points (m = -0.0003, b = 1.48). Unlike for stronger storms, we do not see the strongest GW activity near the end of storm lifetime.